AD-778 964

IGNITION OF HYPERGOLIC LIQUID PROPELLANTS AT LOW PRESSURE

Michel A. Saad, et al

Santa Clara University

Prepared for:

Air Force Office of Scientific Research

March 1974

SECURITY CLASSIFICATION OF THIS PAGE (When Data Entered)

REPORT DOCUMENTATION PAGE

READ INSTRUCTIONS BEFORE COMPLETING FORM

1. REPORT NUMBER: AFOSR - TR - 74 - 0758	2. GOVT ACCESSION NO.
3. RECIPIENT'S CATALOG NUMBER: AD-778964	
4. TITLE (and Subtitle): IGNITION OF HYPERGOLIC LIQUID PROPELLANTS AT LOW PRESSURE	5. TYPE OF REPORT & PERIOD COVERED: FINAL
	6. PERFORMING ORG. REPORT NUMBER
7. AUTHOR(s): MICHEL A SAAD GENE J ANTONIDES SAMUEL R GOLDWASSER	8. CONTRACT OR GRANT NUMBER(s): AFOSR-73-2498
9. PERFORMING ORGANIZATION NAME AND ADDRESS: UNIVERSITY OF SANTA CLARA DEPARTMENT OF MECHANICAL ENGINEERING SANTA CLARA, CALIFORNIA 95053	10. PROGRAM ELEMENT, PROJECT, TASK AREA & WORK UNIT NUMBERS: 681308 9711-01 61102F
11. CONTROLLING OFFICE NAME AND ADDRESS: AIR FORCE OFFICE OF SCIENTIFIC RESEARCH/NA 1400 WILSON BOULEVARD ARLINGTON, VIRGINIA 22209	12. REPORT DATE: March 1974 13. NUMBER OF PAGES: 36
14. MONITORING AGENCY NAME & ADDRESS (if different from Controlling Office)	15. SECURITY CLASS. (of this report): UNCLASSIFIED 15a. DECLASSIFICATION/DOWNGRADING SCHEDULE

16. DISTRIBUTION STATEMENT (of this Report)

Approved for public release; distribution unlimited.

17. DISTRIBUTION STATEMENT (of the abstract entered in Block 20, if different from Report)

18. SUPPLEMENTARY NOTES

19. KEY WORDS (Continue on reverse side if necessary and identify by block number)

IGNITION
HYPERGOLIC
LIQUID PROPELLANTS
EVAPORATION
VAPORIZATION
KINETICS
LOW PRESSURE

20. ABSTRACT (Continue on reverse side if necessary and identify by block number)

Fluids which ignite readily at atmospheric pressure do not necessarily react at low pressures, such as in space. It is only indirectly, through the effect on rates of energy release and energy absorption, that the ignition behavior of a hypergolic liquid is influenced by ambient pressure. Therefore emphasis is placed on determining how pressure affects the rates at which energy is released, absorbed, and distributed. The ignition phenomenon has been examined experimentally in a test facility, where it is possible to establish the relationship between small changes in physical environment and changes in the ignitability of

DD FORM 1 JAN 73 1473 EDITION OF 1 NOV 65 IS OBSOLETE

UNCLASSIFIED
SECURITY CLASSIFICATION OF THIS PAGE (When Data Entered)

hypergolic liquids. Ignition at low pressure was investigated with theoretical techniques, applying thermochemistry and chemical kinetics to establish rates of energy release; evaporation studies to indicate rates of energy absorption; and heat transfer to clarify the rate of distribution of energy within a propellant droplet. While the work has centered about the ignition of hydrazine containing hypergolic liquids at low pressure, the attempt has also been made to develop concepts which apply to ignition of other fluids ~~too~~.

IGNITION OF HYPERGOLIC LIQUID PROPELLANTS AT LOW PRESSURE

Michel A. Saad
Gene J. Antonides
Samuel R. Goldwasser

March 1974

FINAL REPORT

AFOSR Grant ~~68-1478~~ 73-2498
Project 9711-01

Research sponsored by Air Force Office of Scientific Research, Office of Aerospace Research, United States Air Force.

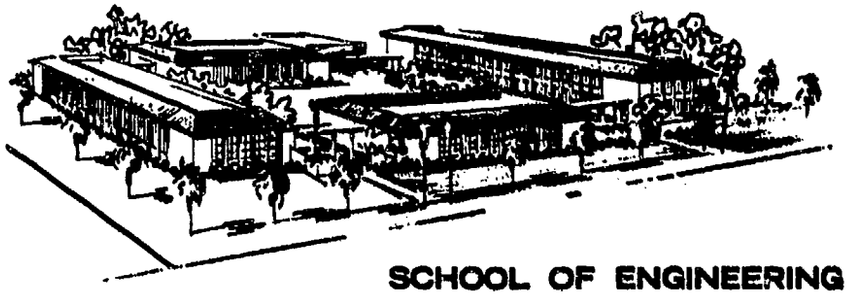

SCHOOL OF ENGINEERING
ENGINEERING AND APPLIED SCIENCE RESEARCH
UNIVERSITY OF SANTA CLARA
SANTA CLARA, CALIFORNIA AREA CODE 408-984-4325

1. Objective

Hypergolic liquids tend to lose their self-igniting capabilities at low pressure. One method of counteracting this loss is to modify the hardware in the region where the jet streams impinge on each other. For example, when a glass cylinder one inch in diameter and six inches in length was positioned concentrically with the axis of the propellant stream, the propellant was found to ignite at pressures considerably lower than those previously observed (Ref. 1). But empirical measures of this type indicate neither the reasons for improvement nor the extent to which the performance can be improved. Consequently, they do not reveal whether the desired performance is attainable even under ideal conditions.

Instead of relying solely on trial and error techniques, it is really necessary to determine, from basic concepts, why hypergolic ignition occurs less readily at low pressure than at high pressure. From such information it may then be possible to devise compensatory schemes, developing ways of assuring ignition at the lowest possible pressures. This report describes results obtained when this type of theoretical approach was applied. The actual procedure employed consisted of a three-step process. First, a simple model of major events assumed to occur during ignition was developed. Second, equations describing these events were established, and these equations were solved for the particular conditions treated by the models. Third, the attempt was made to identify the independent variables which could be controlled and which would permit extension of the ignition range to lower pressures.

Before a hypergolic liquid ignites, a series of events, each lasting only milliseconds, occurs. This sequence is shown schematically in Fig. 1. Impingement, atomization, vaporization, and chemical reaction are shown as the major events leading to ignition. Based on this breakdown, three different models were developed, and each was individually subjected to further analysis in accordance with the process described above.

2. The Kinetics Model

In earlier work (Ref. 1) the attempt was made to show that the total energy released at low pressure is less than at high pressure, in order to prove that the process is self-sustaining only at high pressure. Yet equilibrium thermochemical calculations showed that the process should sustain itself equally well at all pressures. Also, a variety of chemical techniques were applied to analyze the condensed products found in the chamber after ignition was attempted (Ref. 2 and 3). Here, too, chemicals formed at low pressure did not appear significantly different from those at high pressure.

While end products are significant in affecting the ignition process, it has become clear that the rate of formation of end products is even more significant. For the rate at which the liquid decomposes, compared with the rate at which it vaporizes, determines whether the decomposition proceeds rapidly or slowly, if at all. Both decomposition and vaporization are rate processes, there is activation energy associated with each, and the two processes compete against each other for activation energy. Since the rate of vaporization of a liquid depends upon the ambient pressure, this model implicitly incorporates

pressure as a variable. Based on this model, the attempt is then made to calculate time-temperature relationships in a droplet before ignition occurs.

But these time-temperature calculations cannot be readily performed. Values of major parameters in the rate equations, particularly activation energies, are virtually unknown. The only data available is that which states that some particular reactant liquids ignited (or failed to ignite) when mixed in the laboratory under certain particular laboratory conditions. The approach taken, therefore, was to assume values of constants in the rate equations; then, to calculate the resulting time-temperature patterns; finally, to pick out those calculated time-temperature results that match the observed patterns of ignition (or non-ignition) of the measured periods of time, concluding that the corresponding constants were appropriate and could then be used in further calculations as desired. The following propellants were treated in this way: UDMH/N_2O_4, MMH/N_2O_4, N_2H_4/N_2O_4, and N_2H_4/HNO_3. Figure 2 shows typical time-temperature curves of droplets 1000 microns in diameter when different amounts of activation energy are available. When the evaporation rate is assumed to be proportional to the second power of diameter (rather than to the second power of mass) there is a resultant change in the shape of the curve. This becomes evident when Fig. 3 is compared with Fig. 2. And, when droplets 50 microns in diameter rather than 1000 microns in diameter are considered there are marked differences in activation energy requirements. This can be seen by comparing Fig. 4 with Fig. 2. These calculations suggest that large particles do not necessarily show the same ignitibility as small particles do. If this is true then ignition of a hypergolic liquid at

low pressure can be encouraged by forming the liquid particles in those sizes which are most ignitible. Therefore particle size should be a major factor affecting the design of equipment upstream of the point of impingement. These are the main results reached at this point in the investigation, and have been reported both in Synoptic form (Ref. 4) and as a complete manuscript (Ref. 5).

The rate of vaporization of a liquid droplet is proportional to some power of particle size, but the value of this exponent is not clearly established. It was necessary for these calculations (Refs. 4 and 5) to assign some value to this exponent. Based on the particular value assigned to this exponent, ignitibility appears to vary inversely with particle size. When a more appropriate value for this exponent is used, this conclusion perhaps may be confirmed. Yet, it is conceivable that the reverse condition may, in fact, be applicable, or that the most ignitible droplets are those in a certain narrow size range. Until calculations with the "correct" exponent are performed, the relationship between size of particle and ignitibility will continue to remain unclear.

The appropriate value of this exponent can be determined by laboratory measurement. A method of evaluating this exponent for any liquid was developed, and a report describing this method has been written (Ref. 6). The evaluation of rate constants of evaporation is also treated in this report. In Fig. 5, the measured diameter history of an evaporating droplet of hydrazine is shown. It is clear from Fig. 5 that a non-linear relationship appears. But the measured values can be plotted in a different way, with diameter raised to some power (in this case the second power) so that a straight line results, as

shown in Fig. 6. When a straight line is obtained, it is then possible to deduce the exponent involved which relates evaporation rate with particle size.

The rate of vaporization of a spherical droplet is shown by the following differential equation:

$$\frac{d(N/N_o)}{dt} = - k \cdot (\frac{D}{D_o})^{\alpha}$$

where N refers to the mass of the droplet, k is the rate constant, D is the diameter, the subscript o refers to initial values, and α is an exponent which makes the equation appropriate for each set of measured data. Figure 7 shows curves of diameter versus time for different values of the exponent α. A straight line is obtained, in a plot of diameter versus time, only when the exponent α is 2. However, straight-line relationships can be obtained when the diameter, raised to the power whose value is $(3-\alpha)$ is plotted against time, although when α is 3 then a straight-line relationship is obtained only if the logarithmic function of diameter is plotted against time. These are shown in Fig. 8, 9, and 10, for values of the exponent α in the range between 0 and 6.

In practice, both the value of the exponent α and the rate constant k can be determined from measured values of diameter, and time, of an evaporating droplet. This is done by proceeding in the reverse direction, namely, plotting diameter, raised to some power, against time, where the particular power that yields a straight line relationship serves as the indicator of the value of the exponent α and of the rate constant k. Further details of the method are presented in Ref. 6.

3. The Temperature-Distribution Model

As part of the effort to improve the ignitibility of hypergolic liquids at low pressure, this investigation turned to calculating temperatures in a propellant droplet. In this model there is heat generated within the propellant droplet, there is heat conduction within the droplet, and there is loss of mass from the droplet as liquid vaporizes from the surface. Because heat is assumed to be generated uniformly throughout such a droplet, while vapors are released only at the surface, a temperature gradient exists in the droplet with the highest temperature at the center. It is conceivable that the temperature at the center of a droplet can be significantly higher than at the surface so that liquid at the center is more ignitible than is liquid at the surface. The difference in ignitibility cannot be estimated, however, until the difference in temperature can be determined.

The heat flow equation for such a droplet, expressed in spherical coordinates, is:

$$\frac{k}{r^2}\frac{\partial}{\partial r}\left(r^2\frac{\partial T}{\partial r}\right) + Q = \rho\ c_p\frac{\partial T}{\partial t} \qquad 0 \leq r < a,\ t \geq 0$$

where k is the thermal conductivity, r is the radius, T is the temperature, Q is the rate of heat generated per unit volume, ρ is the density, c_p is the specific heat, t is the time, and a is the instantaneous outside radius.

The droplet model assumes a constant surface temperature, so that the heat lost by evaporation is equal to the heat conducted to the surface from within the droplet,

$$\rho\lambda\frac{da}{dt} = k\frac{\partial T}{\partial r} \qquad r = a,\ t \geq 0$$

where λ is the latent heat of vaporization and where the surface temperature is assumed to remain constant.

A search of the literature for a solution to the heat flow equation yielded only Awberry's solution (1927). He considered a droplet in which heat is being generated, but where there is no evaporation of liquid. Awberry reported the radial temperature distribution to be:

$$T = T_s + \frac{G(a^2 - r^2)}{6\alpha} + \frac{1}{r} \sum_{\nu=1}^{\infty} N_\nu e^{-\nu^2\pi^2 \alpha t/a^2} \sin \frac{\nu\pi r}{a}$$

where

$$N_\nu = (-1)^\nu \left[\frac{2Ga^3}{\nu^3\pi^3\alpha} - \frac{2a(T_i - T_s)}{\nu\pi}\right]$$

and where T_s is the surface temperature, G is the heat generation term, a is the outside radius, r is the radial position, α is the thermal diffusivity, t is the time and T_i is the initial temperature. Awberry did not even consider vaporization, and therefore did not take into account any change of radius due to vaporization.

Therefore, a method was developed based on finite-difference techniques to calculate not only time-temperature relationships but also evaporation-rate information. The model used in these calculations is shown in Fig. 11. Before the equations were transposed into finite-difference form, they were converted to a non-dimensionalized form. In this way non-dimensional solutions, which are of more general utility, could be obtained.

The equations were non-dimensionalized by defining the following quantities:

$$C = \frac{k}{a_i^2 C_p Q}, \quad r' = \frac{r}{a_i}, \quad T' = \frac{C_p T}{\lambda}, \text{ and } t' = \frac{Qt}{\rho\lambda}$$

where a_i is the outside radius initially. After these substitutions are made, the heat transfer rate within the droplet is expressed by:

$$C \frac{1}{r'^2} \frac{\partial}{\partial r'} \left(r'^2 \frac{\partial T'}{\partial r'}\right) + 1 = \frac{\partial T'}{\partial t'}$$

A further substitution is:

$$u' = r' T'$$

This leads to $$C \frac{\partial^2 u'}{\partial r'^2} + r' = \frac{\partial u'}{\partial t'} \qquad 0 \leq r' < a,\ t' \geq 0$$

At the surface, the following applies:

$$\frac{da'}{dt'} = C \frac{\partial T'}{\partial r'} \qquad r' = a',\ t' \geq 0$$

In Figs. 12, 13, and 14 temperature histories of three points in the droplet are plotted along with the radius history of the droplet. Figure 12 applies when C = .01, Fig. 13 when C = .1, and Fig. 14 when C = 1.0. These apply when the surface temperature is the same as the initial temperature. Figure 15 presents time-temperature and time-radius data when the surface temperature is different from the initial temperature, where the difference is expressed by the quantity $(c_p T_i/\lambda) - (c_p T_s/\lambda)$.

A paper describing this work will be submitted for publication. Early work on this subject was reported in Ref. 7.

4. The Pressure-Distribution Model

Also affecting the ignitibility of a propellant is the local pressure in the propellant liquid after the streams of liquid impinge on each other. High pressures, even if local, should increase degree of mixing of the reactant liquids and the ignitibility of the propellant.

As a first step toward showing a relationship between pressure distribution and propellant ignitibility, a simplified model was assumed. Two circular jets opposing each other and having the same velocity were considered. The flow was assumed to be inviscid, incompressible

and irrotational. First, streams of equal diameter, velocity and dynamic pressure were treated. A digital computer program was written, using a finite-difference method to solve for the flow streamlines, jet surface contour, and interface pressure distribution (Ref. 8). The jet surface contour and flow streamlines calculated by this program are shown in Fig. 16. Second, two jets of equal velocity and dynamic pressure, but unequal diameter, were considered, as shown in Fig. 17. Streamlines at various locations were then calculated in Fig. 18. Interface pressure distribution and velocities are shown in Fig. 19 for both cases where the jets are equal and, also, where the jets are unequal. A detailed description of the computer program is available at the University of Santa Clara.

After solutions for the two axisymmetric cases were obtained, a new computer program was begun to calculate the flow pattern of two equal-diameter, equal-velocity circular jets impinging at angles other than 180 degrees. This is a more difficult problem because it involves a third dimension with an additional degree of freedom. An initial surface contour is assumed, and the velocity potential values on that surface are calculated by applying a known boundary condition. The interior values of velocity potential are then found by a numerical relaxation method, using the Laplace equation in finite-difference form. A second surface boundary condition is then applied to determine whether the assumed jet surface contour is correct. If the boundary condition is not satisfied, the computer program modifies the assumed surface contour until both boundary conditions are satisfied. The solution is then complete for the velocity potential and surface contour. Gradients of the velocity potential can be taken along the impingement surface to

determine the velocity distribution there and, through the Bernoulli equation, the pressure distribution can be determined. A preliminary case, that of impingement at 180 degrees, was solved with this three-dimensional computer program.

Since values of jet surface contours must be supplied initially to the program, an experimental apparatus was built to measure surface contours. Unfortunately, the program could not be completed before termination of the contract. If this work work were completed, it would contribute significantly to solutions of three-dimensional flow problems.

There have been requests for reprints, for more details about the work done, for a copy of the axisymmetric computer program, and for information on the status of the three-dimensional program.

5. Conclusions

Efforts in this project have been devoted to improving the ignitibility of hypergolic liquid propellants at low pressures. In earlier work, trial and error methods were shown to be remarkably effective. In subsequent work, the same goal was pursued, but the effort consisted of work of a more theoretical nature, attempting to understand the reason for the loss of ignitibility at low pressure and for the improvements obtained by empirical methods. These led to studies in which certain events in the ignition phenomena were simulated. In one simulation study, only vaporization and chemical decomposition were assumed to occur, and in another study it was assumed that only vaporization, heat generation, and heat conduction occur. Both efforts have pointed to the recommendation that more attention be paid to particle size as a factor affecting ignitibility. Another study indicated that further attention also be paid to the angle of impact and the pressure of the impinging jet streams.

Further improvements in ignitibility of hypergolic liquids at low pressure are destined to be achieved. It is not clear, however, whether they will be achieved through the recommendations presented here or even through the models proposed in this research effort. But the approach attempted here, of relating experimental observations with fundamental aspects of the ignition phenomenon, should lead to significant improvements in performance of hypergolic liquid propellants at low pressures.

REFERENCES

1. Saad, M. A., and S. R. Goldwasser, "Role of Pressure in Spontaneous Combustion", AIAA Journal, Vol. 7, No. 8, Aug. 1969, pp. 1574-1581.

2. Saad, M. A., and M. B. Detweiler, "Analysis of N_2H_4-RFNA Reaction Product", AIAA Journal, Vol. 7, 1969, pp. 1588-1592.

3. Saad, M. A., M. B. Detweiler, and M. A. Sweeney, "Analysis of Reaction Products of Nitrogen Tetroxide with Hydrazines under Non-Ignition Conditions", AIAA Journal, Vol. 10, 1972, pp. 1073-1078.

4. Saad, M. A., and S. R. Goldwasser, "Time-Temperature Simulation in Low-Pressure Ignition of Hypergolic Liquids", AIAA Journal, Vol. 12, No. 1, Jan. 1974 (Synoptic).

5. Ibid., National Technical Information Service, U.S. Department of Commerce, Document N73-30865 (Backup).

6. Goldwasser, S. R., and M. A. Saad, "Evaluation of Constants in Droplet Evaporation - Rate Equation", Mechanical Engineering Dept., University of Santa Clara, Oct. 1973.

7. Saad, M. A., and Antonides, G. J., "Heat Flow in a Reacting Drop with Constant Surface Temperature", Mechanical Engineering Dept., University of Santa Clara, Oct. 1971.

8. Saad, M. A., and Antonides, G. J., "Flow Pattern of Two Impinging Circular Jets", AIAA Journal, Vol. 10, No. 7, July 1972, pp. 929-931.

FIGURES

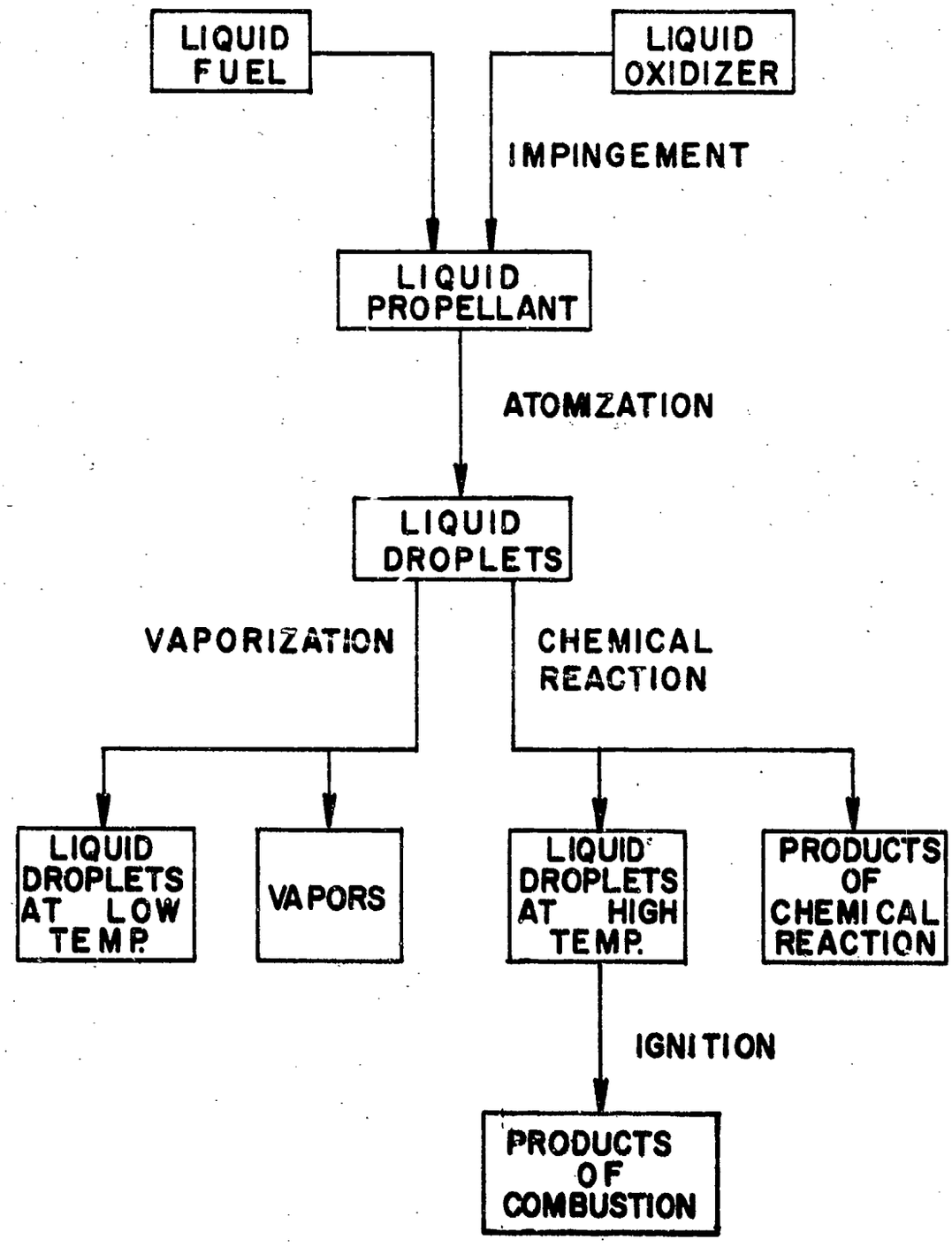

FIG. 1: SEQUENCE OF EVENTS IN HYPERGOLIC IGNITION

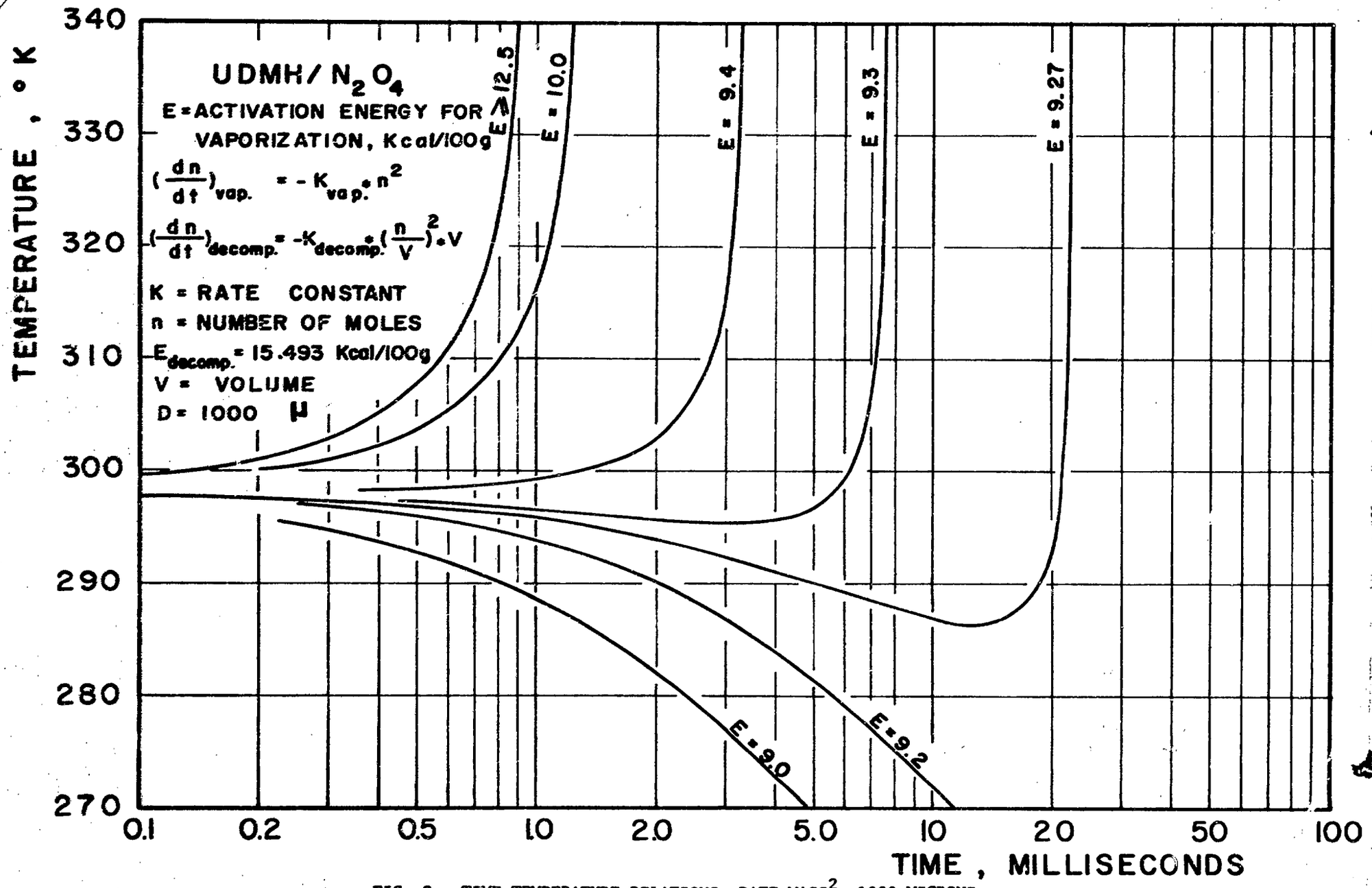

FIG. 2: TIME-TEMPERATURE RELATIONS, RATE MASS^2, 1000 MICRONS

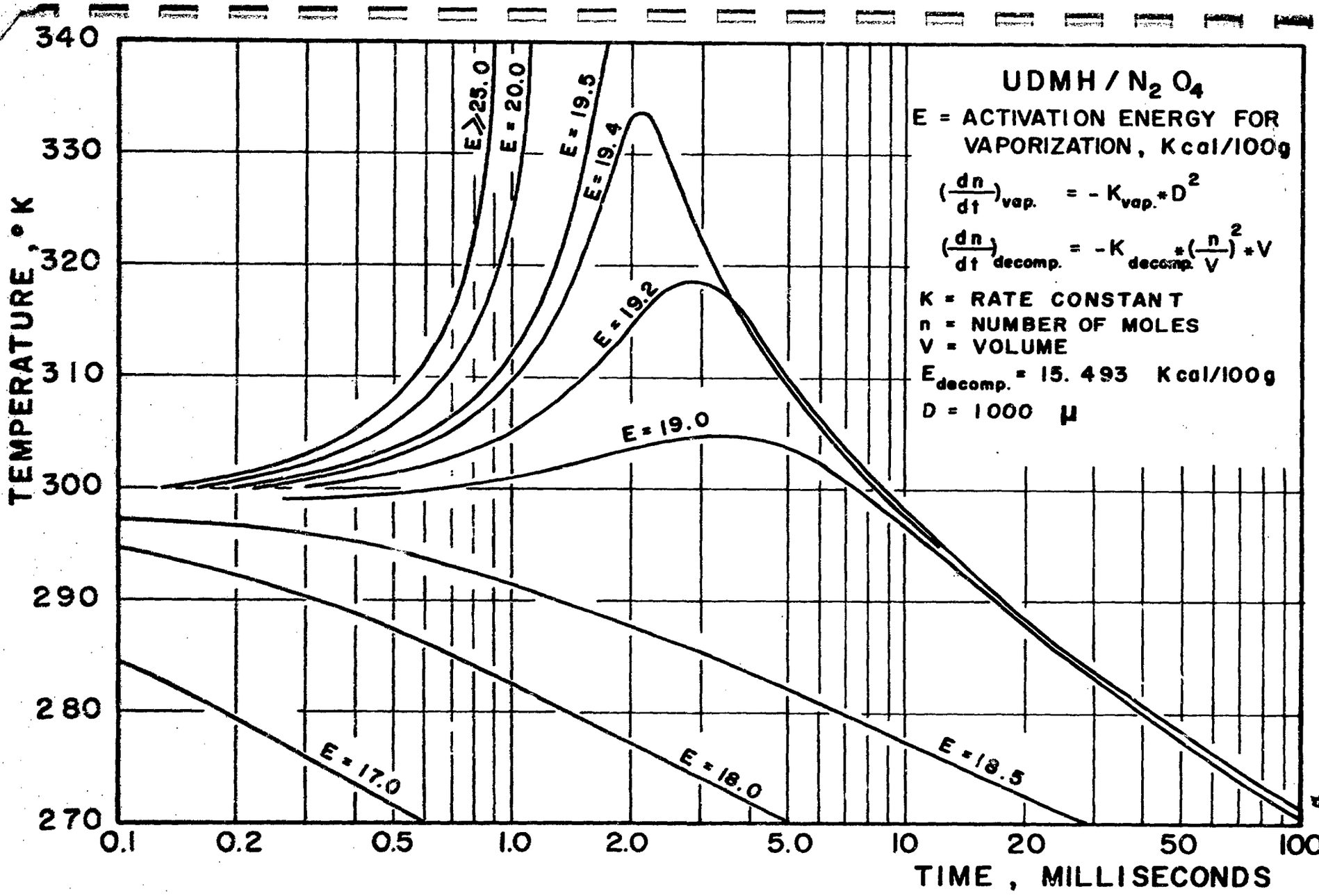

FIG. 3: TIME-TEMPERATURE RELATIONSHIPS, RATE DIAMETER^2, 1000 MICRONS

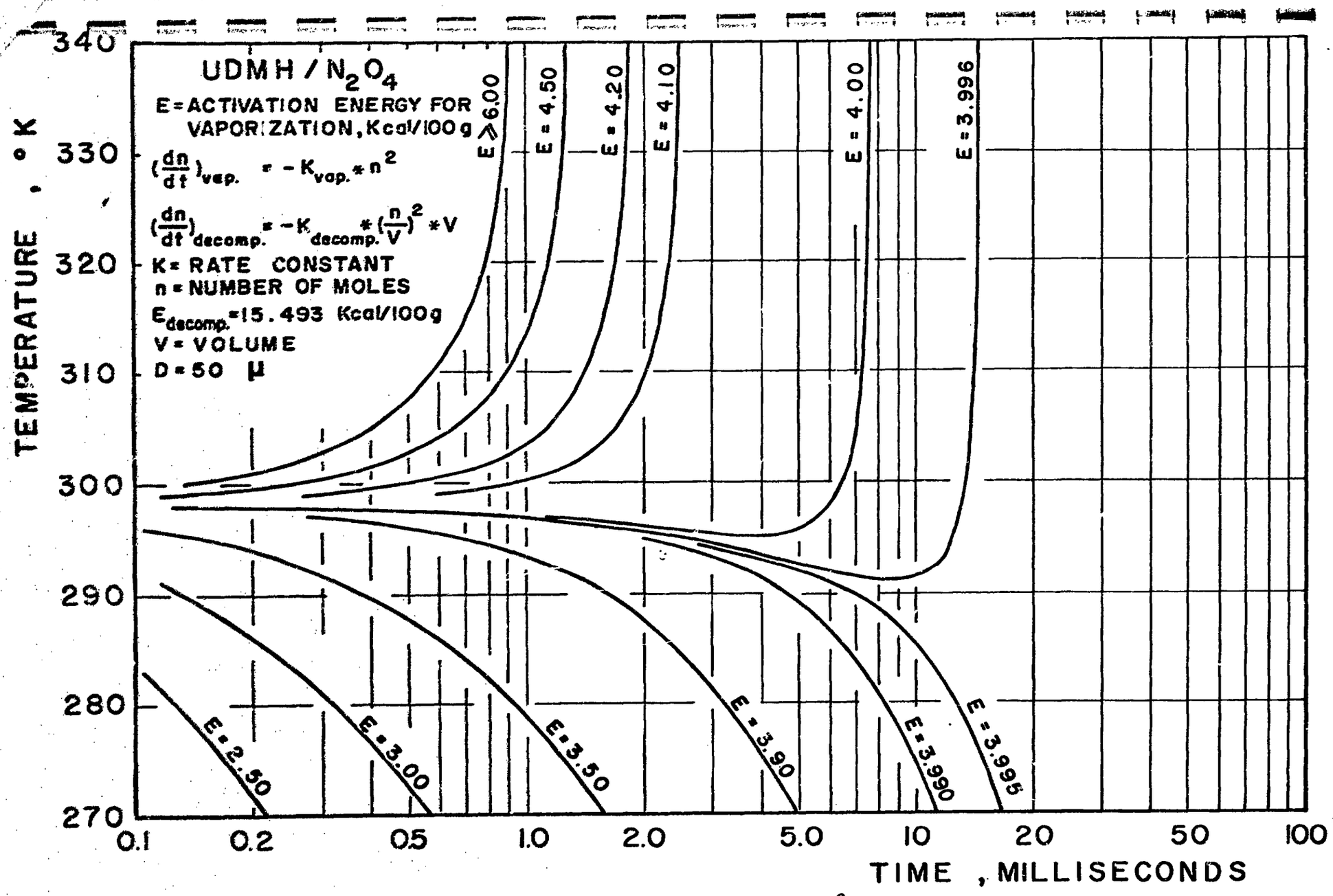

FIG. 4: TIME-TEMPERATURE RELATIONSHIPS, RATE MASS^2, 50 MICRONS

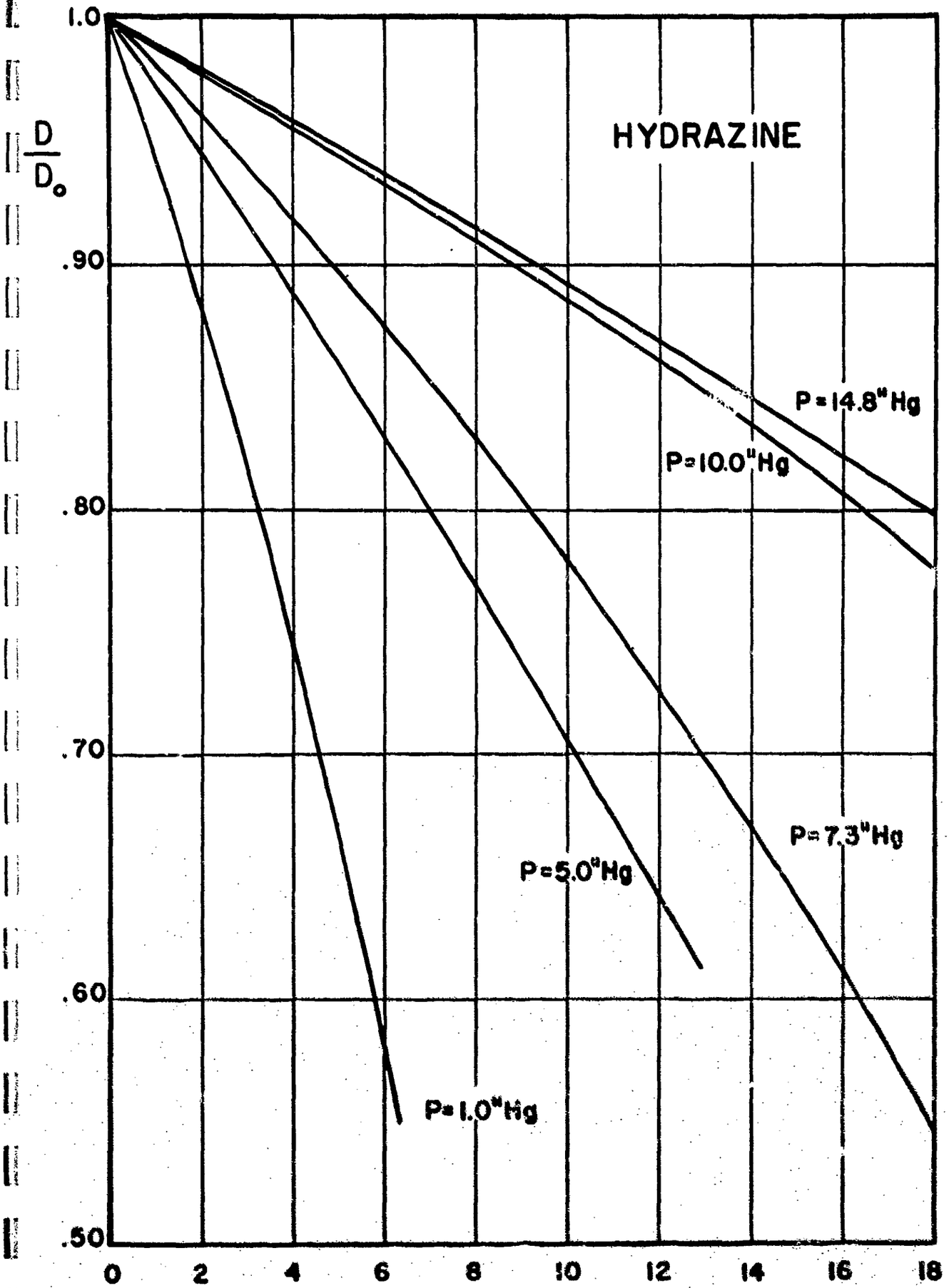

FIG. 5: MEASURED VALUES OF DIAMETER VS. TIME, HYDRAZINE

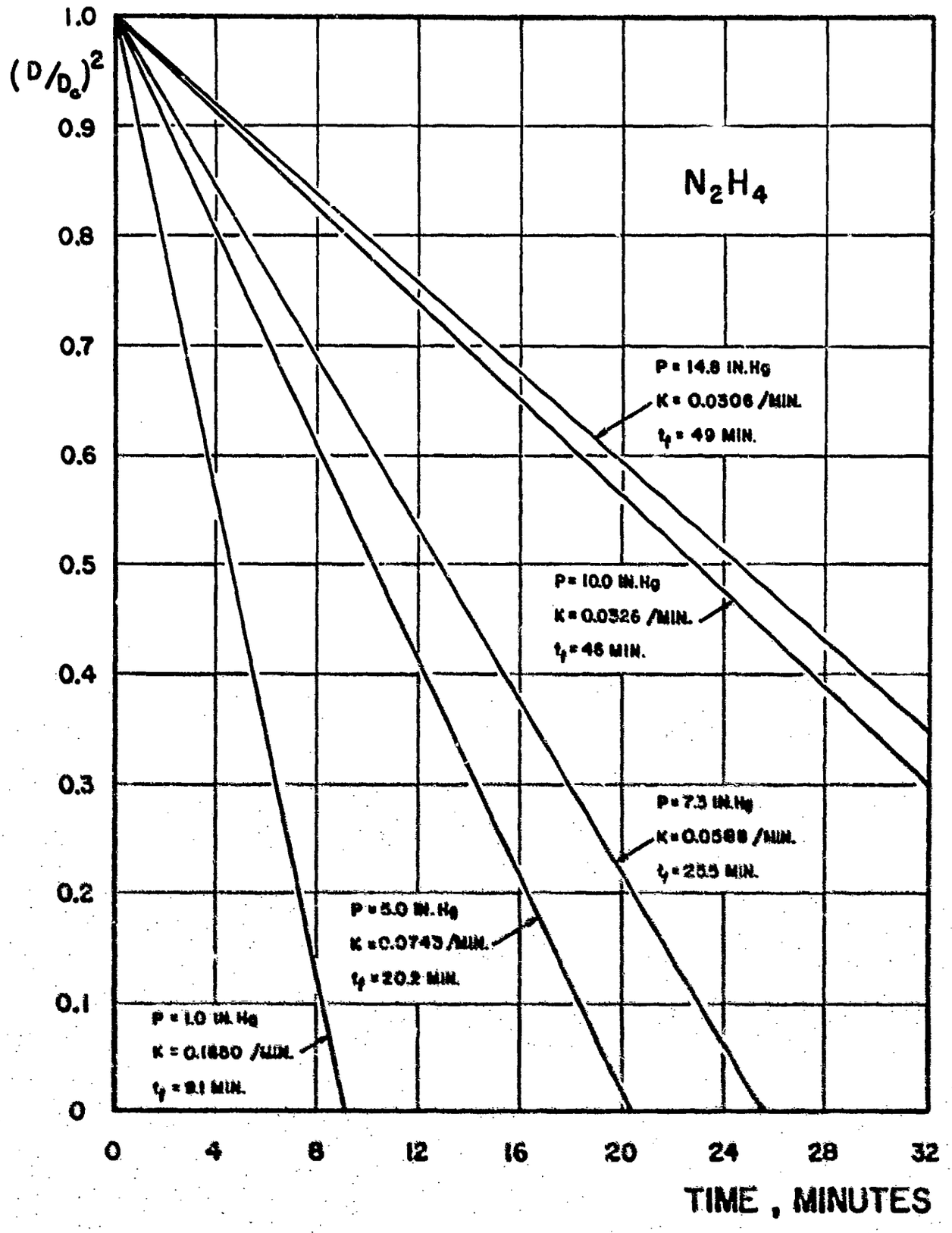

FIG. 6: MEASURED VALUES OF DIAMETER^2 VS. TIME, HYDRAZINE

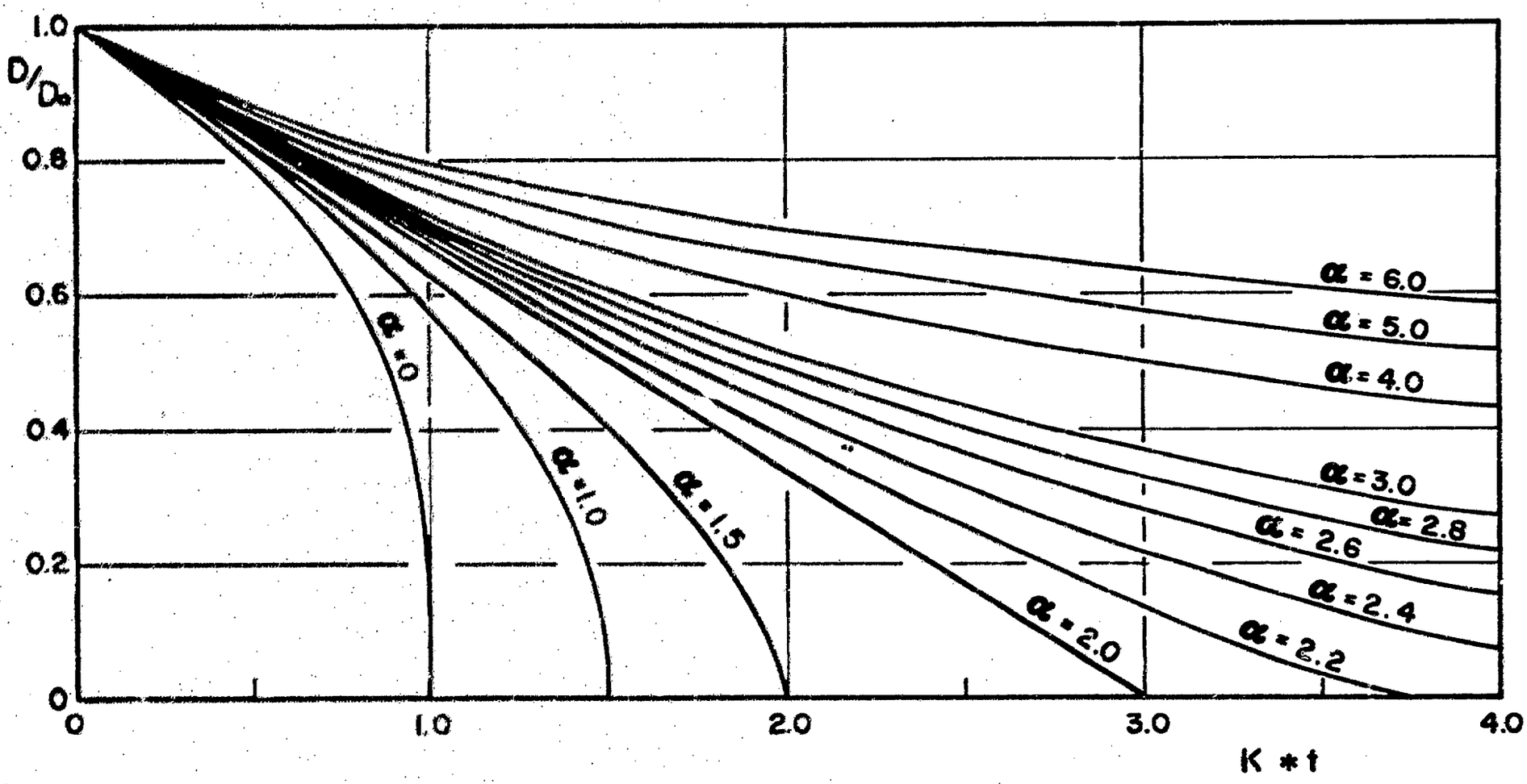

FIG. 7: DIAMETER VS. TIME FOR VARIOUS ALPHA VALUES

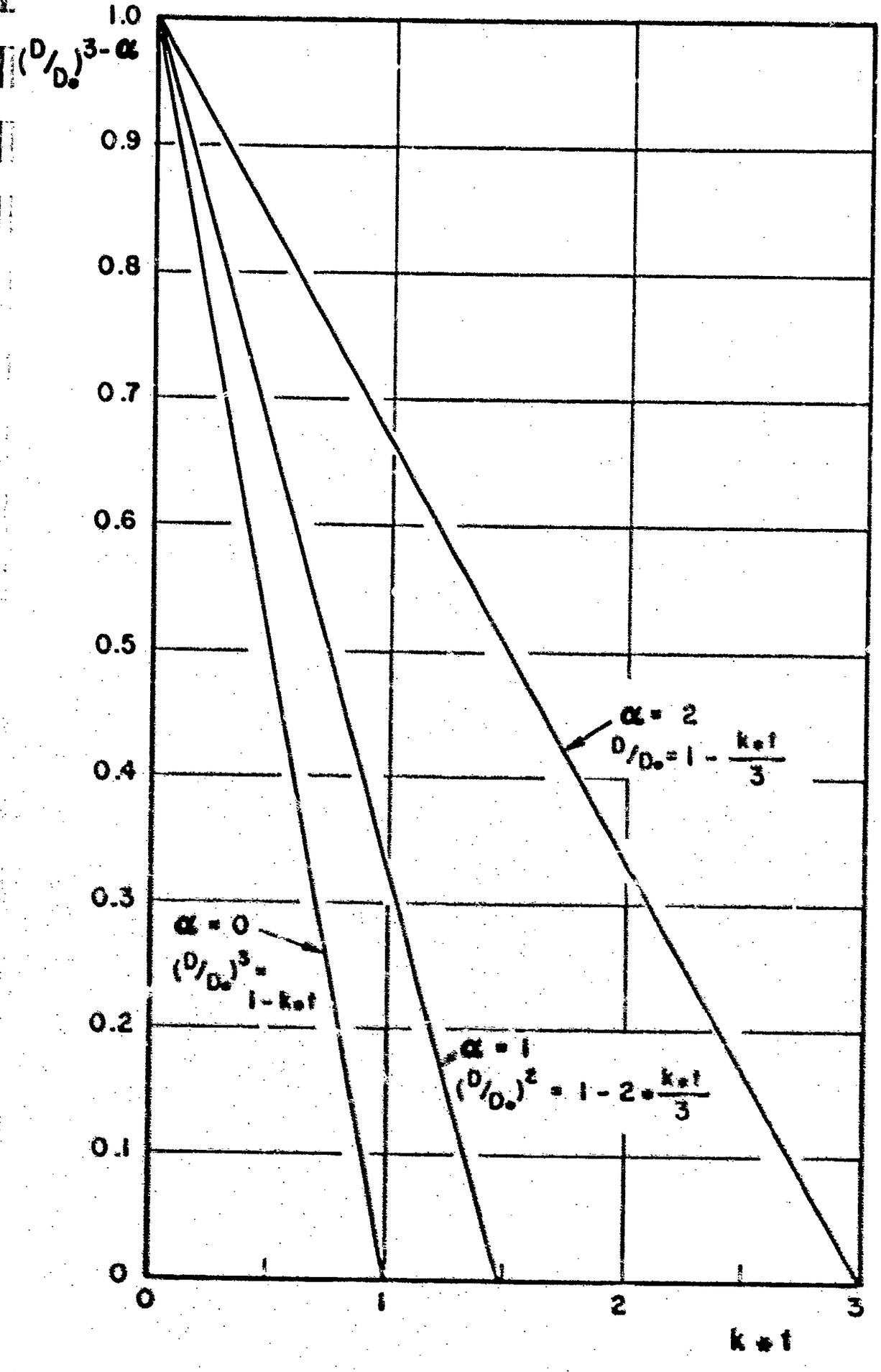

FIG. 8: STRAIGHT-LINE PLOTS, DIAMETER$^{3-\alpha}$ VS. TIME WHEN $\alpha = 0, 1, 2$

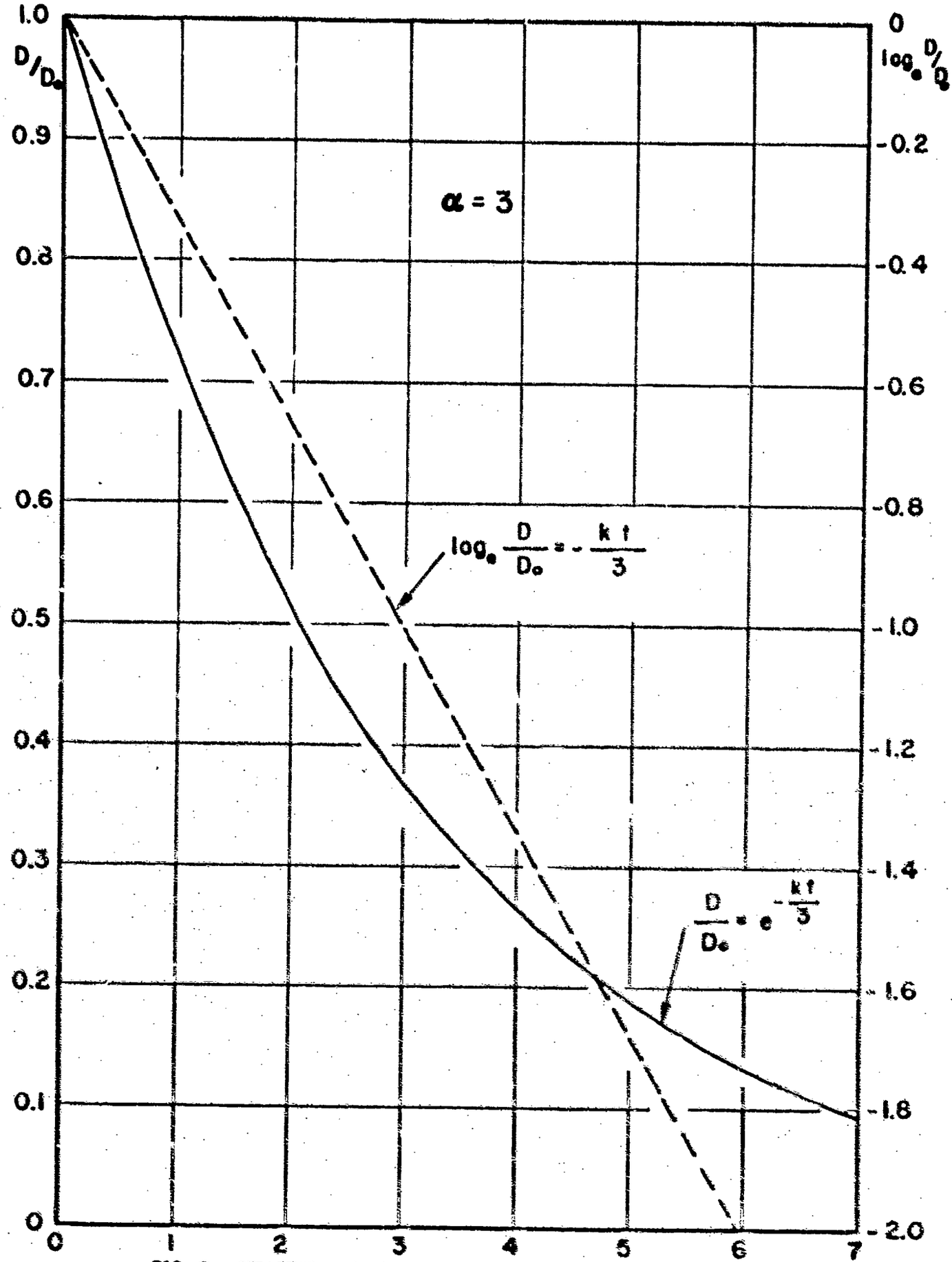

FIG. 9: STRAIGHT-LINE PLOTS, LOG DIAMETER VS. TIME WHEN α = 3

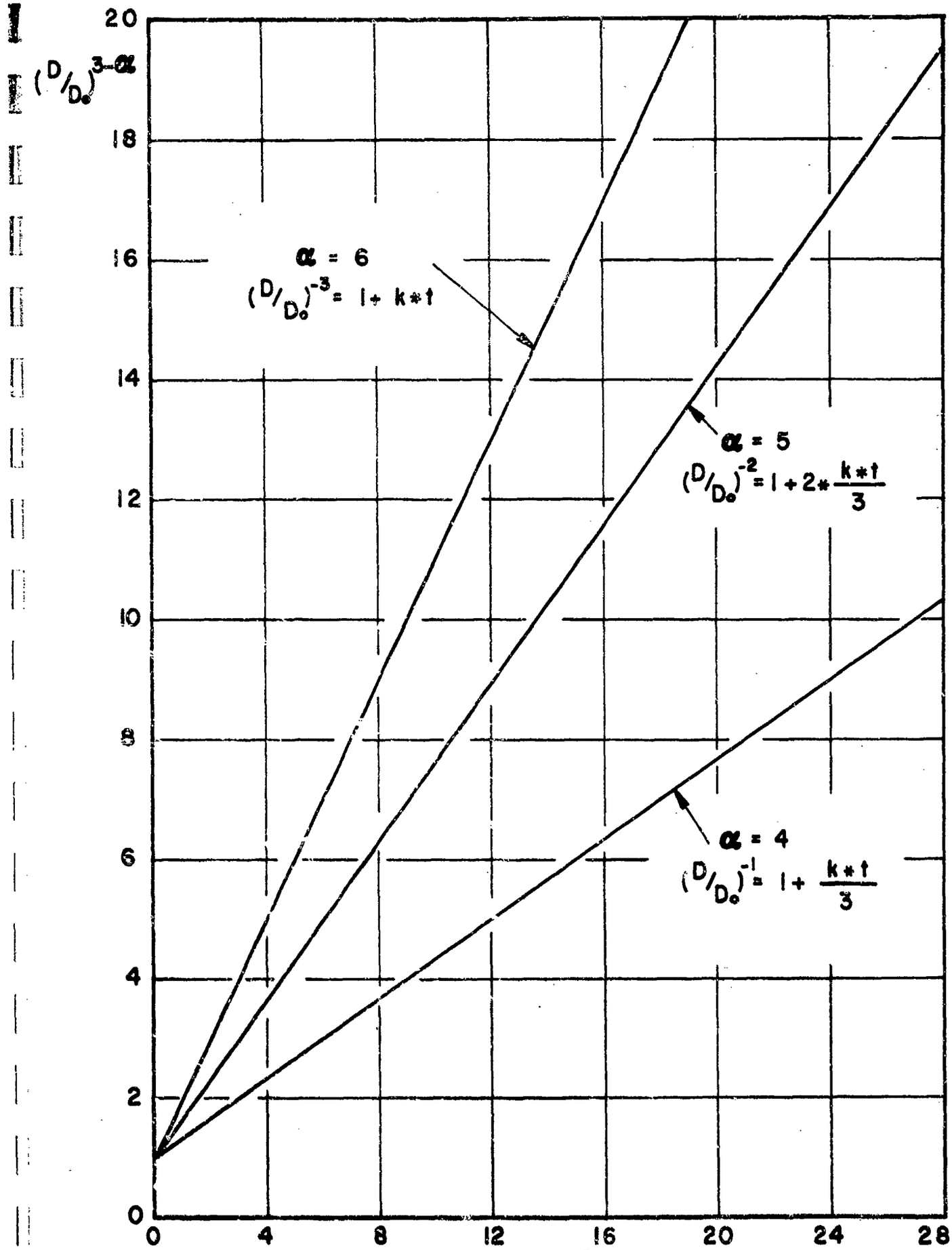

FIG. 10: STRAIGHT-LINE PLOTS, DIAMETER$^{3-\alpha}$ VS. TIME WHEN $\alpha = 4, 5, 6$

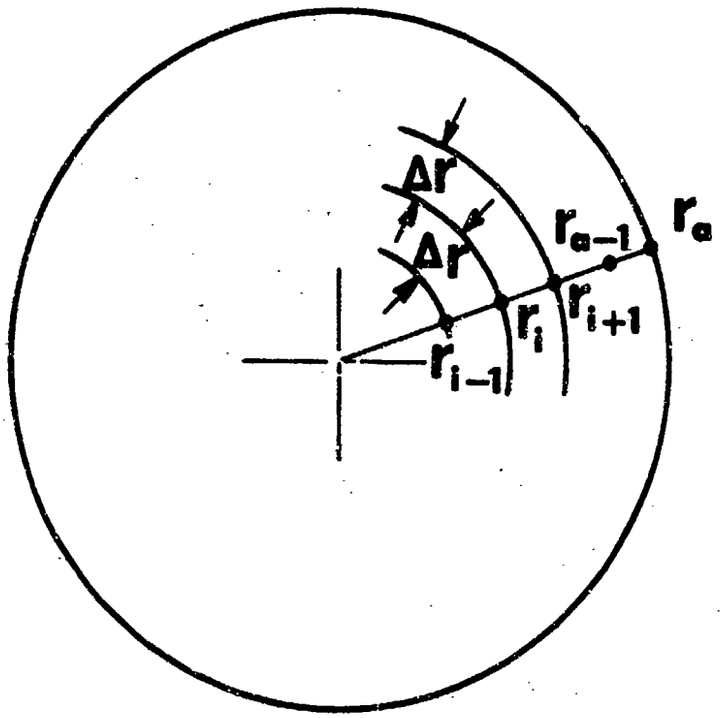

FIG. 11: FINITE-DIFFERENCE MODEL OF DROPLET

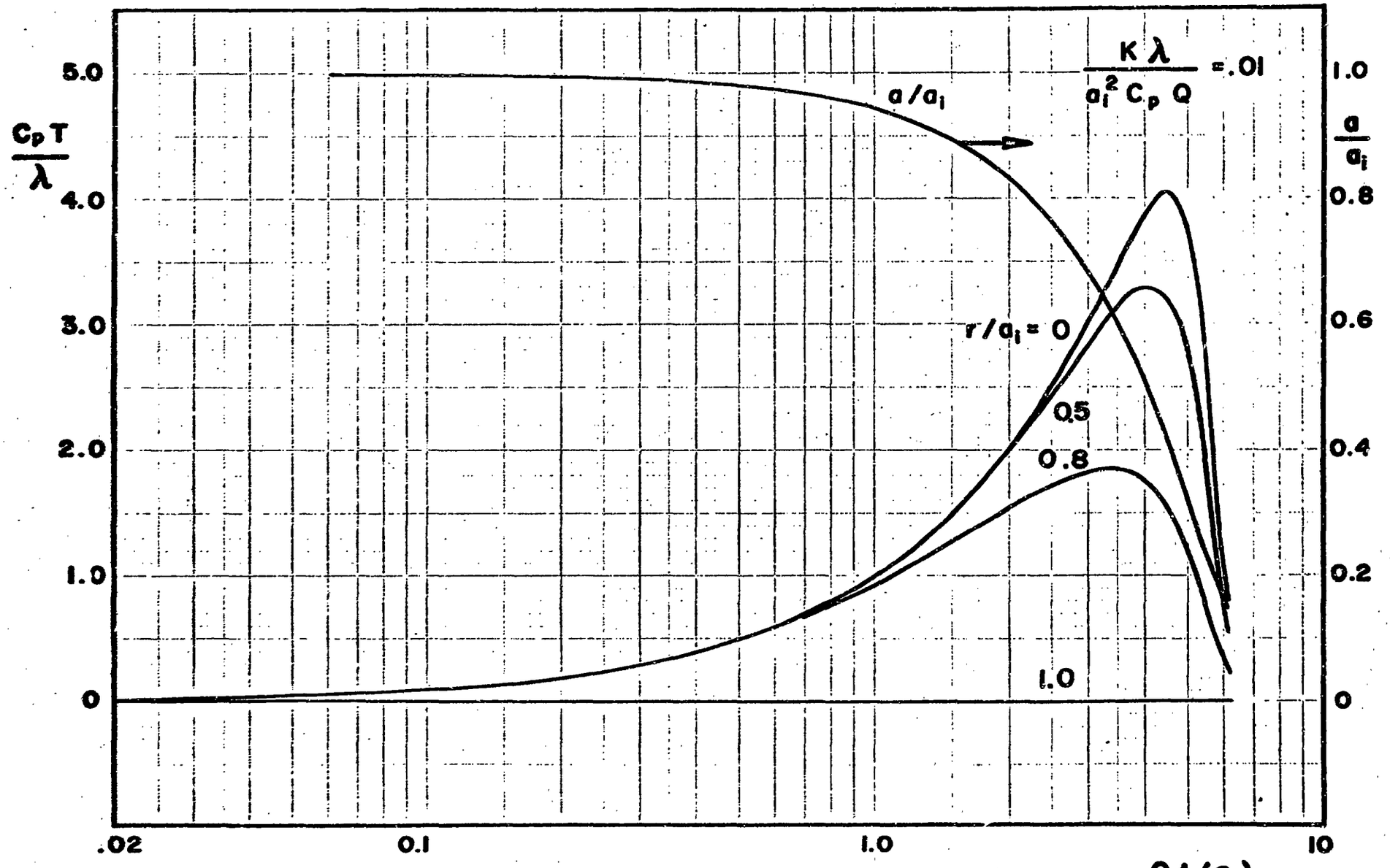

FIG. 12 TEMPERATURE HISTORIES (FOR $r/a_i = 0, 0.5, 0.8, 1.0$) AND RADIUS HISTORY WHEN C = .01

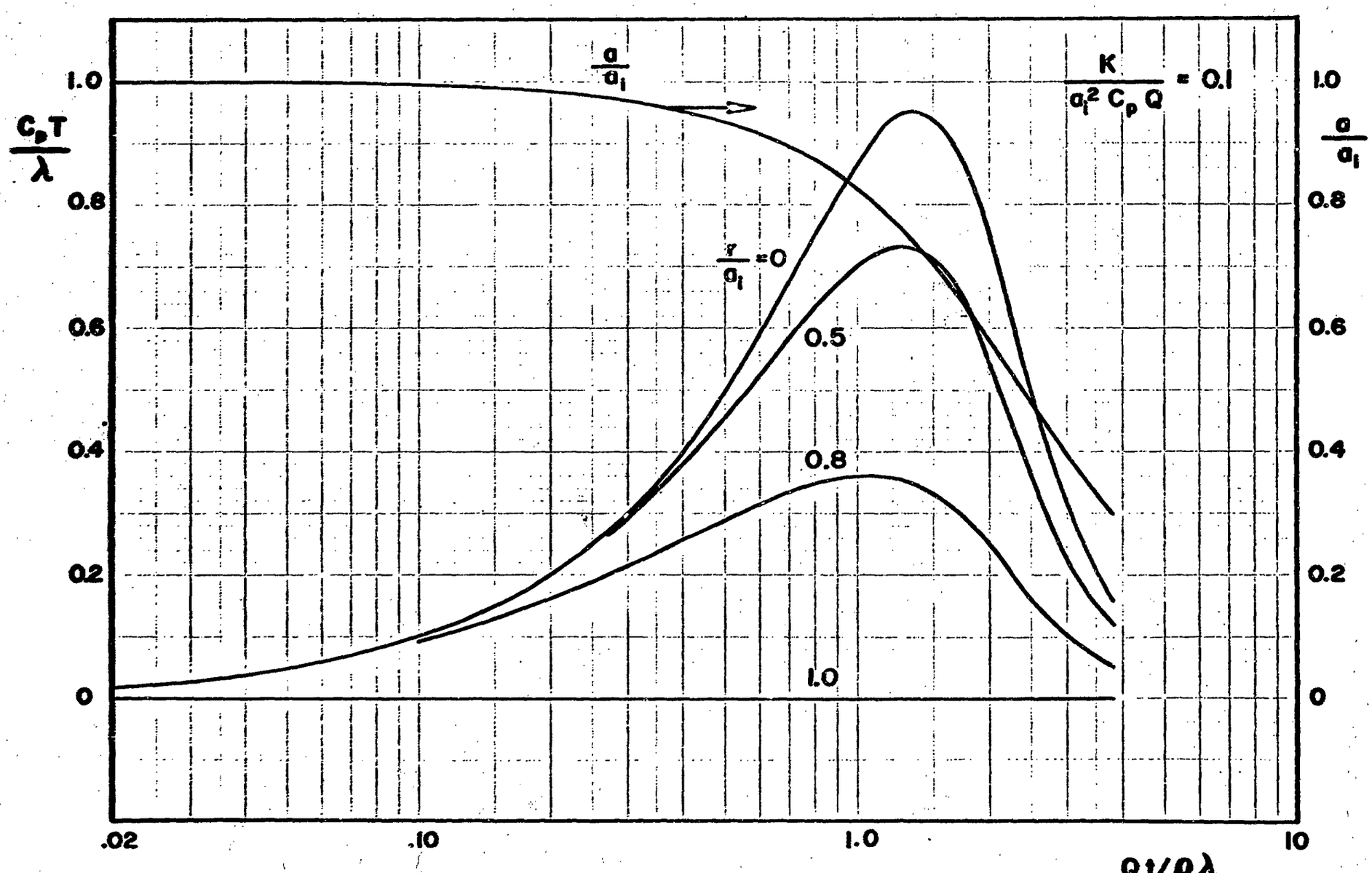

FIG. 13 TEMPERATURE HISTORIES (FOR r/a = 0, 0.5, 0.8, 1.0) AND RADIUS HISTORY WHEN C = 0.1

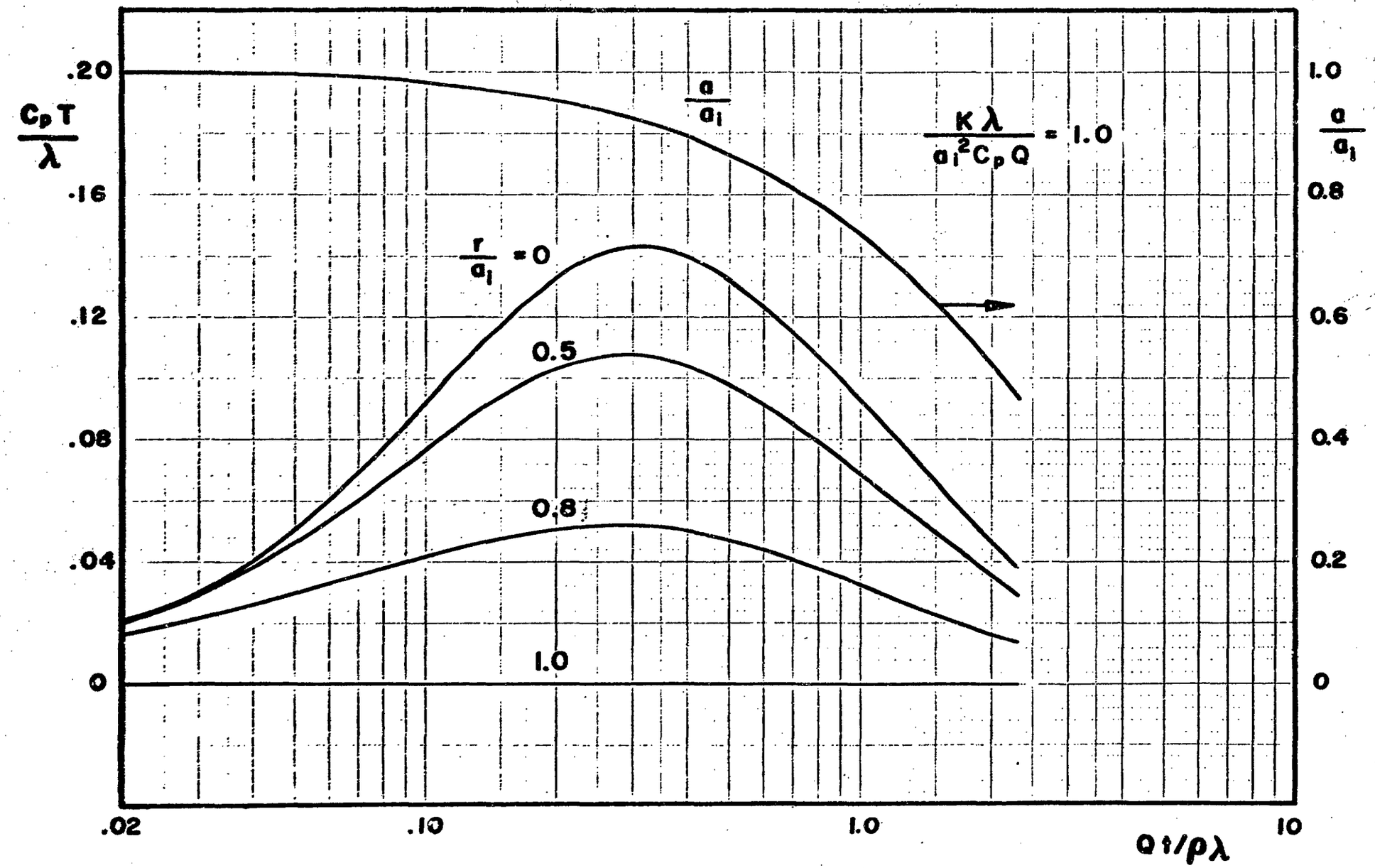

FIG. 14 TEMPERATURE HISTORIES (FOR $r/a_1 = 0, 0.5, 0.8, 1.0$) AND RADIUS HISTORY WHEN C = 1.0

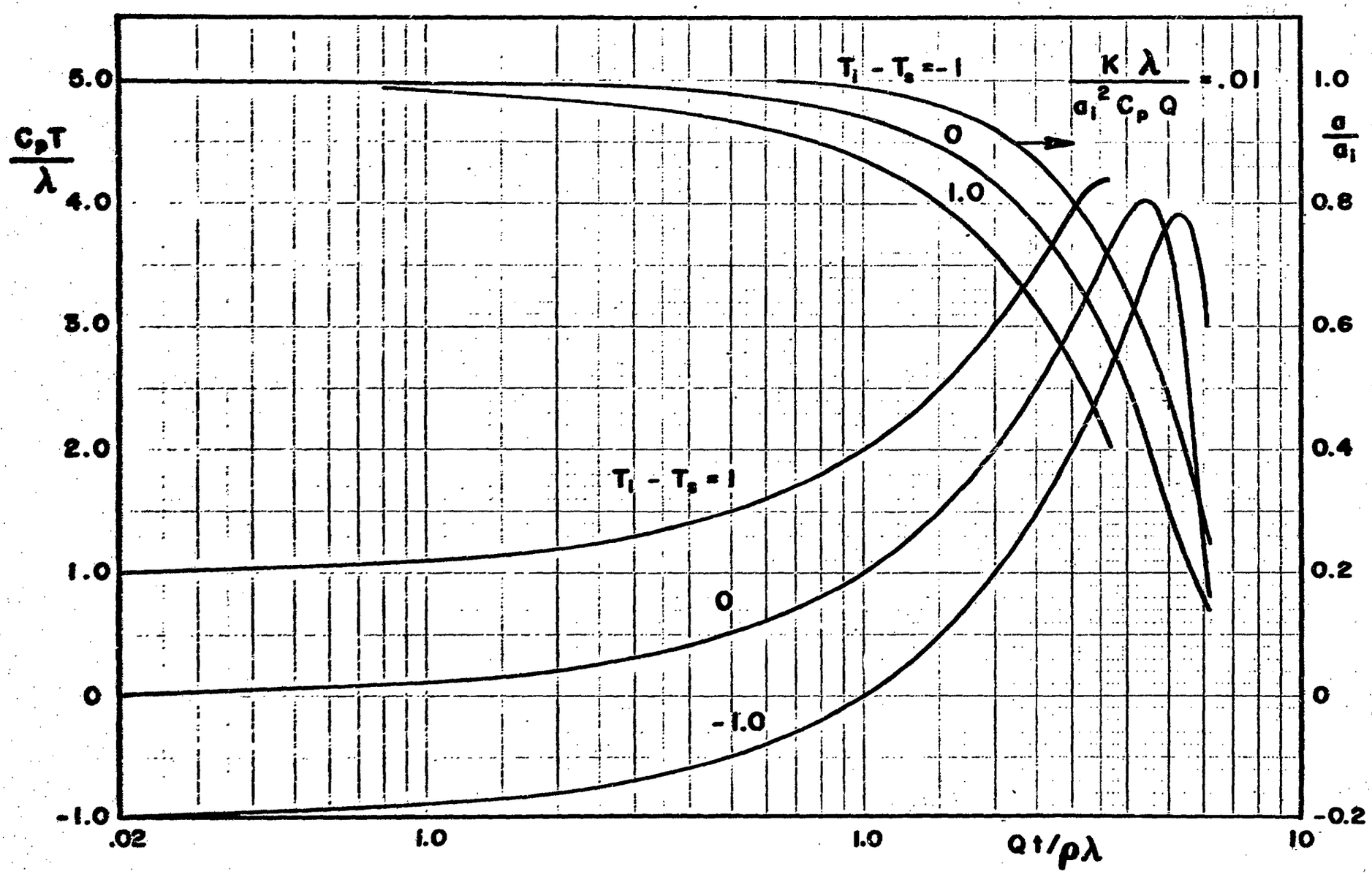

FIG.15 CENTER TEMPERATURE HISTORY ($r/a_i = 0$) & RADIUS HISTORY WHEN $C = .01$ & $T_i - T_s = -1, 0, 1$

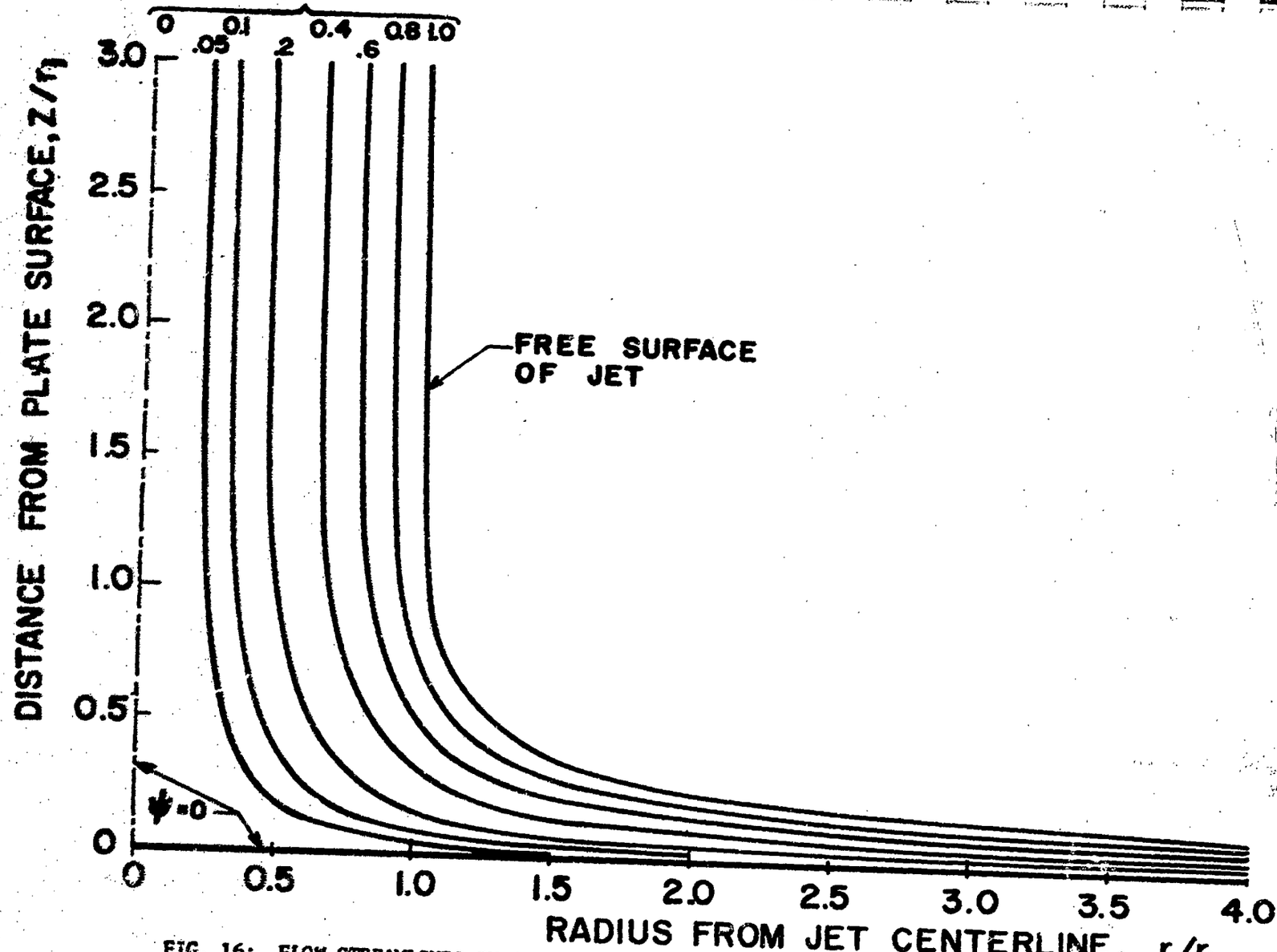

FIG. 16: FLOW STREAMLINES IN CIRCULAR JET IMPINGING ON A PERPENDICULAR SURFACE

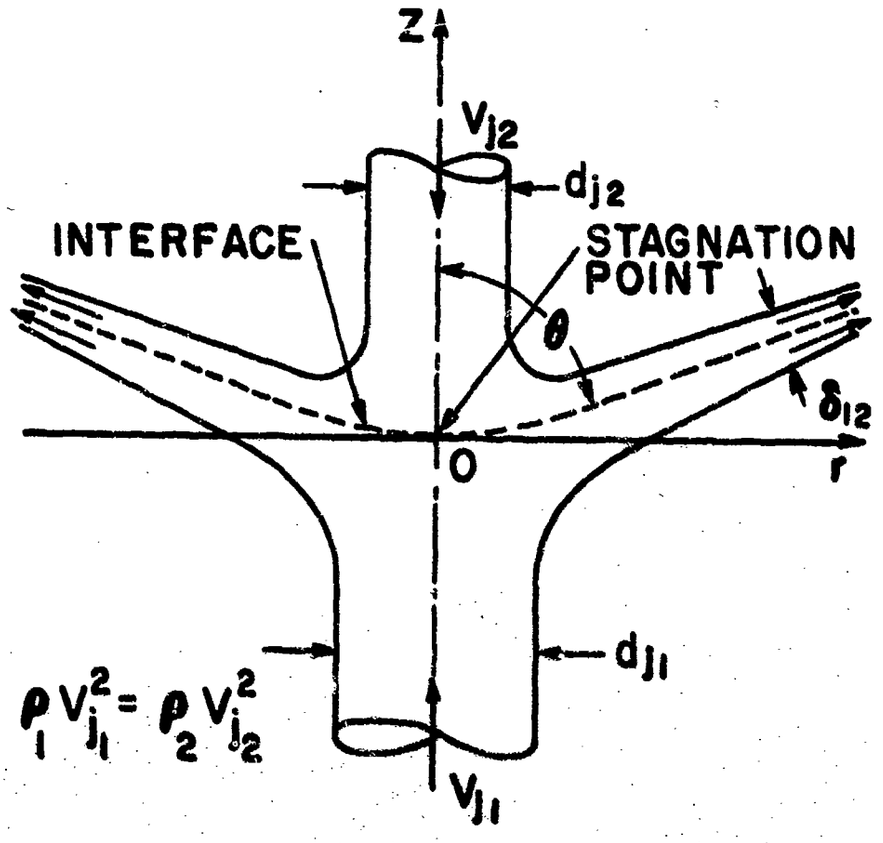

FIG. 17: IMPINGEMENT OF UNEQUAL, OPPOSITE, CIRCULAR JETS

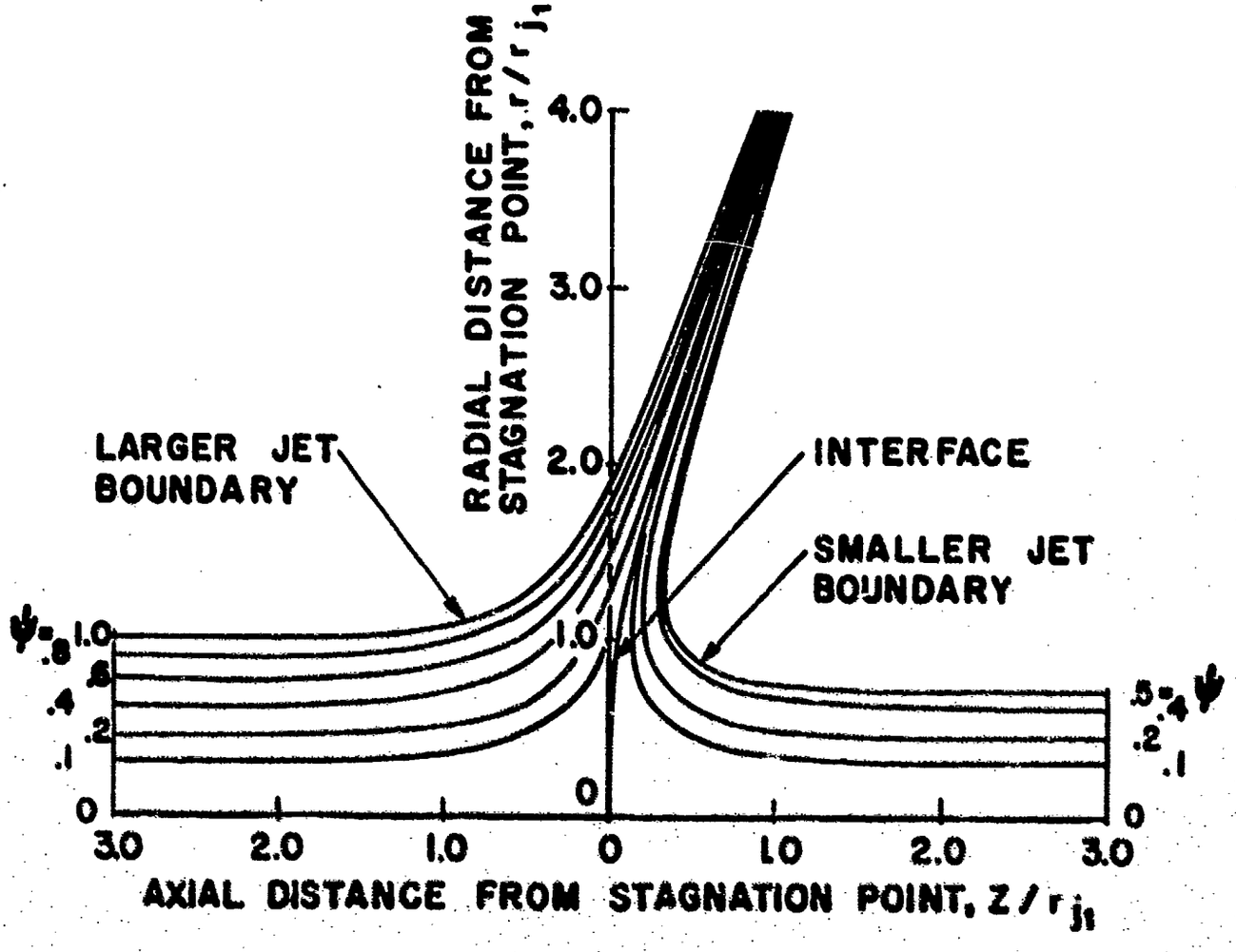

FIG. 16: FLOW STREAMLINES IN UNEQUAL, OPPOSITE, CIRCULAR JETS

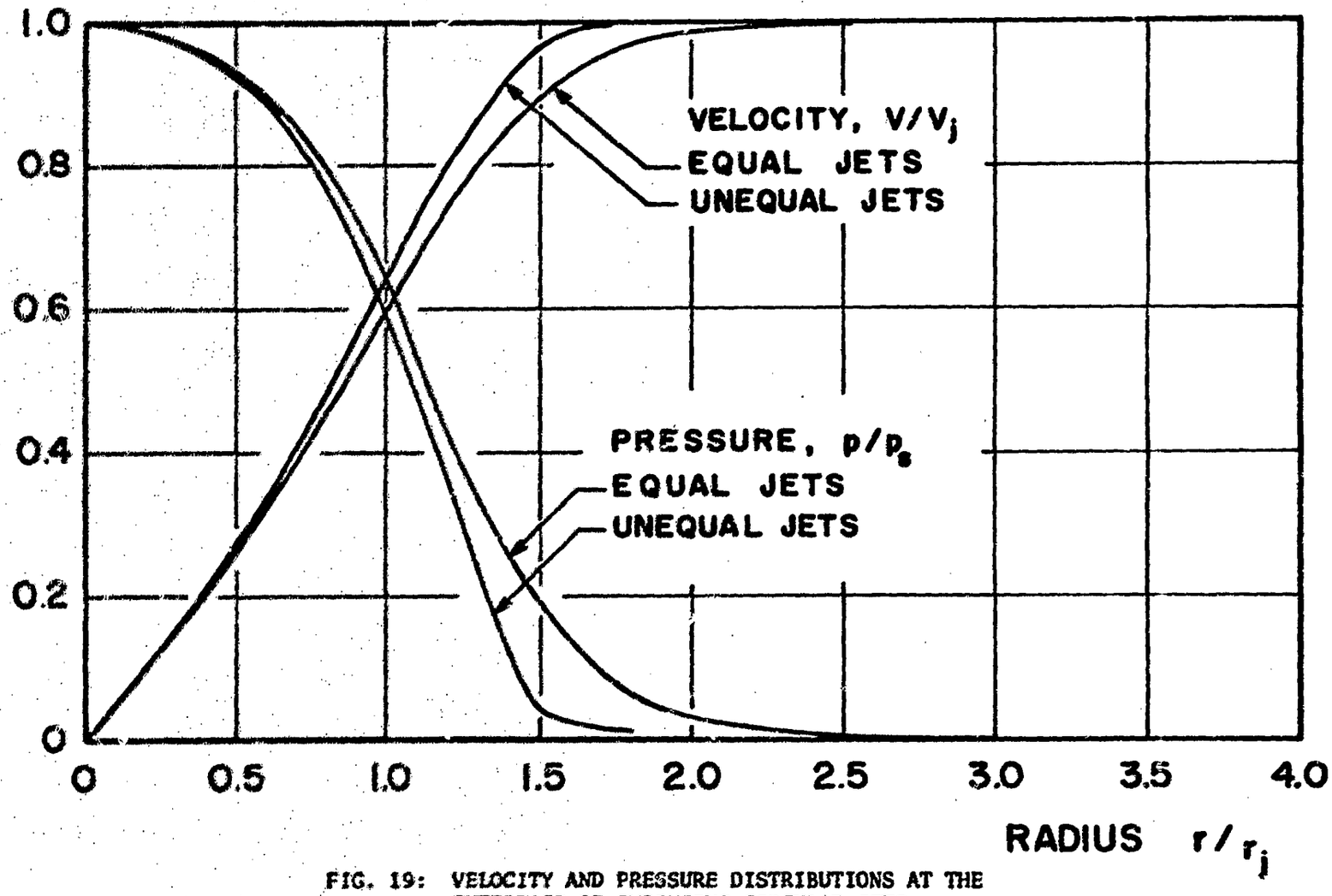

FIG. 19: VELOCITY AND PRESSURE DISTRIBUTIONS AT THE INTERFACE OF IMPINGING CIRCULAR JETS